CONF-860906--21

CONF-860906--21

DE87 004995

TRANSIENT BOWING OF CORE ASSEMBLIES IN ADVANCED LIQUID METAL FAST REACTORS

S. A. Kamal and Y. Orechwa

Applied Physics Division
Argonne National Laboratory
9700 South Cass Avenue
Argonne, IL 60439

DISCLAIMER

TRANSIENT BOWING OF CORE ASSEMBLIES IN ADVANCED LIQUID METAL FAST REACTORS

S. A. Kamal and Y. Orechwa

Applied Physics Division
Argonne National Laboratory
9700 South Cass Avenue
Argonne, IL 60439

ABSTRACT

Two alternative core restraint concepts are considered for a conceptual design of a 900 MWth liquid metal fast reactor core with a heterogeneous layout. The two concepts, known as limited free bowing and free flowering, are evaluated based on core bowing criteria that emphasize the enhancement of inherent reactor safety. The core reactivity change during a postulated loss of flow transient is calculated in terms of the lateral displacements and displacement-reactivity-worths of the individual assemblies. The NUBOW-3D computer code is utilized to determine the assembly deformations and interassembly forces that arise when the assemblies are subjected to temperature gradients and irradiation induced creep and swelling during the reactor operation. The assembly ducts are made of the ferritic steel HT-9 and remain in the reactor core for four-years at full power condition. Whereas both restraint systems meet the bowing criteria, a properly designed limited free bowing system appears to be more advantageous than a free flowering system from the point of view of enhancing the reactor inherent safety.

I. INTRODUCTION

Present LMR core designs in the U.S. focus on concepts which will respond to current perceptions of economic and social realities. This requires cores with a smaller output which, it is felt, are more appropriate in view of the slower growth rate in electricity demand and current financial constraints. In addition, current LMR core design activities have placed emphasis on the maximum enhancement of the inherent reactivity feedbacks and larger thermal inertia of the LMR pool design. It is felt that a demonstrable inherently safe LMR core design should contribute to making nuclear power more socially acceptable and should allow the removal of costly safety systems associated with previous designs -- thereby reducing the cost of the reactor plant.

In the design of LMR cores which maximize the inherent safety features of these reactors, a net negative reactivity insertion during transient events must be assured. The bowing of core assemblies is one of the critical core design elements with respect to its effect on the net reactivity during a transient such as a loss-of-flow. During a loss-of-flow (LOF) transient, the

reactor power-to-flow ratio (P/F) reaches more than twice the value at normal operating conditions. This increase in the P/F raises the duct wall temperatures of the assemblies and introduces temperature gradients across the assemblies. As a result, the core assemblies distort relative to their nominal positions. Assembly bowing, which causes radial outward displacement of the core region, is one of the design features that reduces the core reactivity insertion.

In the present paper, two alternative core restraint systems for a conceptual design of a liquid metal reactor are compared based on their bowing reactivity effect during a LOF transient. The first system includes a restraint ring at the level of the top load pads (TLPs) to control the displacements of the outer-most row of the assemblies. This system is called a limited-free-bowing restraint system. The second system does not include a restraint ring and thus allows the assemblies to freely flower outward during a LOF transient. This system is called a free-flowering restraint system. Except for the restraint ring difference, the two systems are very similar. The systems provide two supports for the assemblies at the lower grid plates and permit interaction between assemblies at the above core load pads (ACLPs) and the TLPs.

II. REACTOR CORE DESIGN

It has recently been shown[1] that there is significant economic and inherent safety potential in core designs with metal-based fuel. Metal fuel has not received widespread attention for large LMFBR application over the last two decades, primarily due to previously unfavorable high burnup fuel performance characteristics and a high mixed mean outlet temperature requirement. Recent developments, however, indicate that metal fuel performance comparable and perhaps even superior to that of oxide fuel can be achieved.[2] Further, calculations indicate that the high thermal conductivity of metal fuel enhances the inherent safety response of the system, especially during loss-of-flow-without-scram transients.[3] Metal fuel also allows for a compact, simplified integral fuel cycle with uranium startup.[4,5]

The analysis of the two core constraint systems is made in the context of a metal fueled 900 MWth liquid metal fast reactor designed to the specifications shown in Table I. The core has a radially-heterogeneous configuration which is shown in Fig. 1. It consists of 102 driver assemblies, 85 blanket assemblies, 12 control assemblies, and 180 reflector assemblies. The approach to shielding in this layout is to use two types of reflector assemblies: 54 steel assemblies in the first row, and 126 assemblies containing B_4C in the last two rows.

The fuel assemblies are designed to take into account the above constraints and are shown in Table II. These are primarily reflected in the choice of the ferritic steel HT-9 as the structural material, and the sizing of the duct and interassembly sodium gap. The fuel is ternary metal U-Pu-Zr, although the core has been designed to neutronically accommodate a startup with U-Zr and the transition to U-Pu-Zr through the recycle of the bred Pu.

The constraints of annual refueling and a peak discharge burnup limit of ~150 MWd/kg limit the driver fuel pin diameter to 0.285 in. The cladding thickness associated with this pin diameter is initially selected as 0.022 in.

which gives a diameter-to-cladding thickness ratio of 13. The relatively high fast fluence of 3.45×10^{23} n/cm^2 in this core dictates the need for a strong duct of 0.140 in. in thickness. This requires a 0.150 in. interassembly gap to accommodate irradiation induced creep and swelling. Due to the use of the low swelling ferritic alloy HT-9 in this core, the duct dilation is due, almost exclusively, to pressure-driven irradiation induced creep. The 0.150 in. interassembly gap accommodates only duct rounding. For the bowing analysis, the fuel, blanket, and control assemblies are assumed to have the same duct designs and therefore identical mechanical behavior. The shield assemblies in the limited-free-bowing system are assumed to be identical to the inner assemblies. In the free-flowering system, however, the shield assemblies have a stiffness that is twice that of the inner assemblies in order to provide more lateral support for the inner assemblies.

III. MODELING

The computer code NUBOW-3D[6] is used to calculate the deflection of the assemblies and the contact forces between them during full power steady state operation and LOF transients. The NUBOW-3D code considers the assemblies in a 30-degree sector of the core. The assembly conditions in the remaining eleven sectors are assumed to be identical to the one analyzed. The assembly configuration and numbering system used in the present analyses are shown in Figure 2. In the vertical direction, the model requires five sets of nodes: geometry, strain, temperature, and flux nodes in addition to load points. The five sets are shown with the corresponding elevations in Figure 3. The number and location of the nodes in the various sets are selected such that the assembly geometry, temperatures, neutron flux, and deformations can be reasonably and accurately described in the vertical direction. For example, the strain nodes are concentrated in the core region where the inelastic strains are most important. The assembly temperatures and neutron fast flux are supplied to the code for each of the six sides of each assembly at the temperature and flux nodes.

In this study, the code takes into account correlations for the irradiation induced creep and swelling. It also allows the displacement-reactivity-worths in two perpendicular directions to be introduced for each assembly. The displacement-reactivity-worths are then combined with the assembly lateral displacements to arrive at the total reactivity change due to bowing of the assemblies,

$$\Delta\rho = \sum_{i=1}^{N} \sum_{j=1}^{M} (wx_{ij}u_{ij} + wy_{ij}v_{ij})\Delta z_{ij}$$

where wx_{ij} and wy_{ij} are the displacement reactivity worths in the x and y directions per unit axial length, u_{ij} and v_{ij} are the lateral displacements, and Δz_{ij} is the incremental axial length. The subscript i indicates the assembly number and the subscript j indicates the geometry node number. M is the number of geometry nodes and N is the total number of core assemblies. The assembly worths are assumed to have a cosine distribution in the vertical direction with peak values at the core mid-plane and null values at the bottom and top of the core. The average values of the distributions are equal to the quantities generated by the neutronic calculations in which a single assembly location is perturbed at a time[7]. The peak values are shown on each assembly

in Figures 4a and 4b. One may notice in these figures that the neutronic model allows assembly displacements that are not constrained by the NUBOW 30-degree model of the core.

The present analysis approximates equilibrium cycle operation in a four batch mode and a fuel residence time of 1168 full power days. The assembly duct temperatures[6] are specified at the beginning-of-equilibrium cycle (BOEC) and end-of-equilibrium cycle (EOEC), with linear interpolation for intermediate times. The neutron fast flux field[7] and the set of displacement-reactivity-worths corresponding to EOEC conditions are used throughout the cycle. LOF transients with P/F varying from one to two are considered in the analysis at both BOEC and EOEC. The rise-to-power transient in which P/F is varied from zero to one is also considered at the two ends of the equilibrium cycle. The temperature field during the transients are derived from the preceding full power condition. The temperatures of the assembly ducts relative to the grid plate temperature are assumed to vary in proportion to the power-to-flow ratio.

IV. RESULTS

The main emphasis in the analysis of the two restraint systems is on the change in the bowing reactivity as P/F increases from one to two during LOF transients. The displacements of the assemblies and the interacting forces between the assemblies are also evaluated to assure that the designs of the restraint systems are feasible. It is important to point out that the present results are for a selected set of design parameters and input data, which are based on preliminary analyses conducted on both restraint systems. These preliminary analyses showed that the amount of the clearances at the load pads and the contact stiffnesses at these pads significantly influence the outcome of the analyses. The clearances are chosen such that for each system the reactivity change is the largest attainable value while the displacements and forces are within acceptable design limits. The clearances and other major design parameters used in the bowing analyses are summarized in Table III.

The LOF transients are calculated at two time points, BOEC and EOEC. The changes in core reactivity are shown as a function of P/F in Figures 5a and 5b for the limited-free-bowing and free-flowering systems, respectively. The figures depict the reactivity variation at both BOEC and EOEC conditions. The distinct change in the slope of the reactivity curves for the limited-free-bowing system is a result of the changes in the clearance at the load pads. At P/F=1 the clearances diminish as the assemblies become fully compacted and the deformations of the assemblies at larger P/F values are determined by the dilation and the forces at the load pads. Below P/F=0.8 the system behavior is dominated by the temperature gradient of the assemblies in the core region. The limited-free-bowing system inserts a negative reactivity of about 20 cents as P/F increases from 1 to 2. The free-flowering system, however, inserts only about 9 cents. Based on this comparison, it appears that the limited-free-bowing system can contribute more to the inherent safety of the core in the event of LOF transient.

An examination of the variation of the bowing reactivity from one assembly to another shows that the fuel assemblies at the outer rows (e.g., assemblies 7, 17, 26 and 32) contribute most of the negative reactivity during the LOF transient. This can be attributed to the relatively large

displacement-reactivity-worths of these assemblies. The lateral deformations of these assemblies are also quite similar. The deformations (y-components) of assembly 7 are plotted for P/F=1 and P/F=2 conditions along with the difference between the two conditions in Figures 6a and 6b. The figures illustrate these deformations for the two alternative restraint systems during a LOF transient that occurs at BOEC. With the limited-free-bowing system, the assembly exhibits the largest outward radial displacement in the core region during the transient. This occurs in spite of the TLP inward movement which is largely controlled by the restraint ring. On the other hand, with the free-flowering system, the assembly exhibits the largest outward displacement at the TLP level. In the core region, however, the same assembly shows much smaller outward displacement than at TLP and slightly less than the core region with the limited-free-bowing system. The difference between the two systems in the amount of the outward displacement of the core region is directly related to the difference in the reactivity change during the LOF transient.

The displacements and forces of the various assemblies at the TLPs are illustrated in Figures 7a and 7b for the two systems at the full power BOEC condition. Similarly, the displacements and forces at the EOEC condition are illustrated in Figures 8a and 8b. The limited-free-bowing system shows smaller displacements and larger forces than the free-flowering system. A more detailed comparison between the two systems is given in Table IV. The contact forces at the BOEC conditions are smaller than at EOEC, particularly for the limited-free-bowing system. This decrease in the forces occurs mainly in the first two-hundred days of operation as a result of creep strain accumulation. The high resistance of the ferritic steel HT-9 to swelling, even in the high fluence environment of the metal-fueled core, prevents a subsequent increase in the contact forces. Table IV also shows estimates for the largest forces required to withdraw any of the assemblies during refueling at EOEC. During full-power condition, the largest displacement of any assembly at TLP level is about 0.5 inch and the contact forces are below 1500 pounds. During refueling, the largest displacement is below 0.25 inch and the largest expected withdrawal force is about 2000 pounds. The level of these displacements and forces appear to be within the acceptable limits of similar designs[6].

V. CONCLUSIONS

It has been shown that a limited-free-bowing core restraint system can be more advantageous than a free-flowering system from the view point of enhancing the inherent response of liquid metal reactor to off-normal transients. During a LOF transient, the limited-free-bowing system controls the deformations of the assemblies such that the assemblies move radially outward in the core region more than in the case of a free-flowering system. The limited-free-bowing system thus inserts more negative reactivity as P/F increases during the transient.

The comparison between the two alternative restraint systems was conducted for feasible core restraint systems and with input data that correspond to a preliminary stage of core design. In a more advanced design stage, the contact stiffness at the load pads could be varied to reflect more precisely the level of core compaction and the type of loading on the pads. With free-flowering restraint systems, the core is less compacted and smaller

contact stiffness may be more appropriate to use in the analysis. This would further reduce the amount of the negative reactivity for this type of restraint system.

VI. REFERENCES

1. Y. I. Chang, J. F. Marchaterre, and R. H. Sevy, "The Integral Fast Reactor Concept," Trans. Am. Nucl. Soc., 47, 293 (1984).

2. L. C. Walters, B. R. Seidel, and J. H. Kittel, "Performance of Metallic Fuels and Blankets in Liquid-Metal Fast Breeder Reactors," Nucl. Technol., 65, 179 (1984)

3. S. F. Su and R. H. Sevy, "Inherent Accommodation of Unprotected Loss-of-Flow Accidents in LMFBRs," Trans. Am. Nucl. Soc., 47, 300 (1984).

4. L. Burris, M. Steindler, and W. Miller, "A Proposed Pyrometallurgical Process for Rapid Recycle of Discharged Fuel materials from the Integral Fast Reactor," Proc. Fuel Reprocessing and Waste Management Meeting, Jackson, Wyoming, August 1984.

5. L. Burris and L. C. Walters, "The Proposed Fuel Cycle for the Integral Fast Reactor," Trans. Am. Nucl. Soc., 49, 90 (1985).

6. J. T. Madell et al., "Core Restraint and Seismic Analysis of Large Heterogeneous Free-Flowering Core Design," Argonne National Laboratory, EPRI NP-1615, November 1980.

7. K. D. Derstine, "DIF3D: A Code to Solve One-, Two-, and Three-Dimensional Finite-Difference Diffusion Theory Problems," Argonne National Laboratory, ANL-82-64, April 1984.

8. K. L. Basehore and N. E. Todreas, "SUPERENERGY-2: A Multiassembly Steady-State Computer Code for LMFBR Core Thermal Hydraulic Analysis," Pacific Northwest Laboratory, PNL-3379, August 1980.

ACKNOWLEDGMENT

The authors thank the ANL colleagues who provided the inputs that made this study possible. D. J. Malloy performed the thermal-hydraulics analysis, H. S. Khalil performed the neutronics analysis to generate the neutron flux, S. T. Yang performed the neutronics analysis to generate the displacement-reactivity-worths, and G. M. Greenman and T. J. Moran took part in updating the NUBOW-3D code. The authors also thank D. C. Wade for reviewing the paper. This work was supported by the U.S. Department of Energy, Nuclear Energy Programs under Contract W-31-109-Eng-38.

TABLE I. General Reactor Specifications

Reactor Power, MWt	900
Core Concept	Heterogeneous
Reactor Outlet Temperature, °C(°F)	510 (950)
Reactor ΔT, °C(°F)	135 (275)
Fuel Residence Time, Cycles	
Driver	4
Internal Blanket	4
Radial Blanket	4
Fuel Material	U-Pu-Zr
Structural Material	HT-9
Cycle Length, days	365
Capacity Factor	80%

TABLE II. Description of Reactor Core and Assemblies

Peak Fast Flux, 10^{15}n cm^{-2} s^{-1}	
BOEC	3.42
EOEC	3.41
Peak Fast Fluence, 10^{23}n cm^{-2}	3.45
Duct Outside Flat-to-Flat, in.	5.911
Duct Wall Thickness**, in.	0.140
Assembly Lattice Pitch, in.	6.061
Total Assembly Length, in.	184
Core Height*, in.	36
Top Plenum*, in.	48
Top Shield*, in.	30
Bottom Shield*, in.	28

Notes: *Driver (Fuel) assemblies.
**All assemblies except radial shields in free-flowering system. The wall thickness of these radial shields is 0.292 inch.

TABLE III. Bowing Analysis Main Input Data

Modulus of Elasticity, lb/in^2	24.2×10^6
Coefficient of Thermal Expansion, /°F	6.65×10^{-6}
Coolant Pressure Difference, lb/in^2	70
Contact Stiffness, lb/in	
Load Pads	3×10^6
Nozzle Supports	1×10^6
Restraint Ring	50×10^6
Height of Load Pads, in.	6
Initial Clearances with Limited-Free-Bowing*, in.	
Nozzle Tip	0.008
Nozzle Support	0.010
ACLP	0.018
TLP	0.010
Restraint Ring	0.060
Initial Clearances with Free-Flowering*, in.	
Nozzle Tip	0.002
Nozzle Support	0.000
ACLP	0.007
TLP	0.005

Note: *Clearances at 70°F

TABLE IV. Comparison Between Limited-Free-Bowing and Free-Flowering Restraint-Systems

	Limited-Free-Bowing	Free-Flowering
Reactivity Change in LOF Transient, cents		
At BOEC	-18.2	- 6.9
At EOEC	-21.0	-10.5
Average	-19.6	- 8.7
Largest Force on Load Pads, lb		
At BOEC	1363	403
At EOEC	365	116
Largest Force on Nozzle, lb		
At BOEC	226	952
At EOEC	41	1152
Largest Withdrawal Force, lb	382	1969
Largest Displacement at TLP, in		
At BOEC*	0.094	0.451
At EOEC*	0.096	0.514
At Refueling	0.128	0.223

Note: *Displacements of control rod ducts are much smaller than the largest displacements of all the ducts.

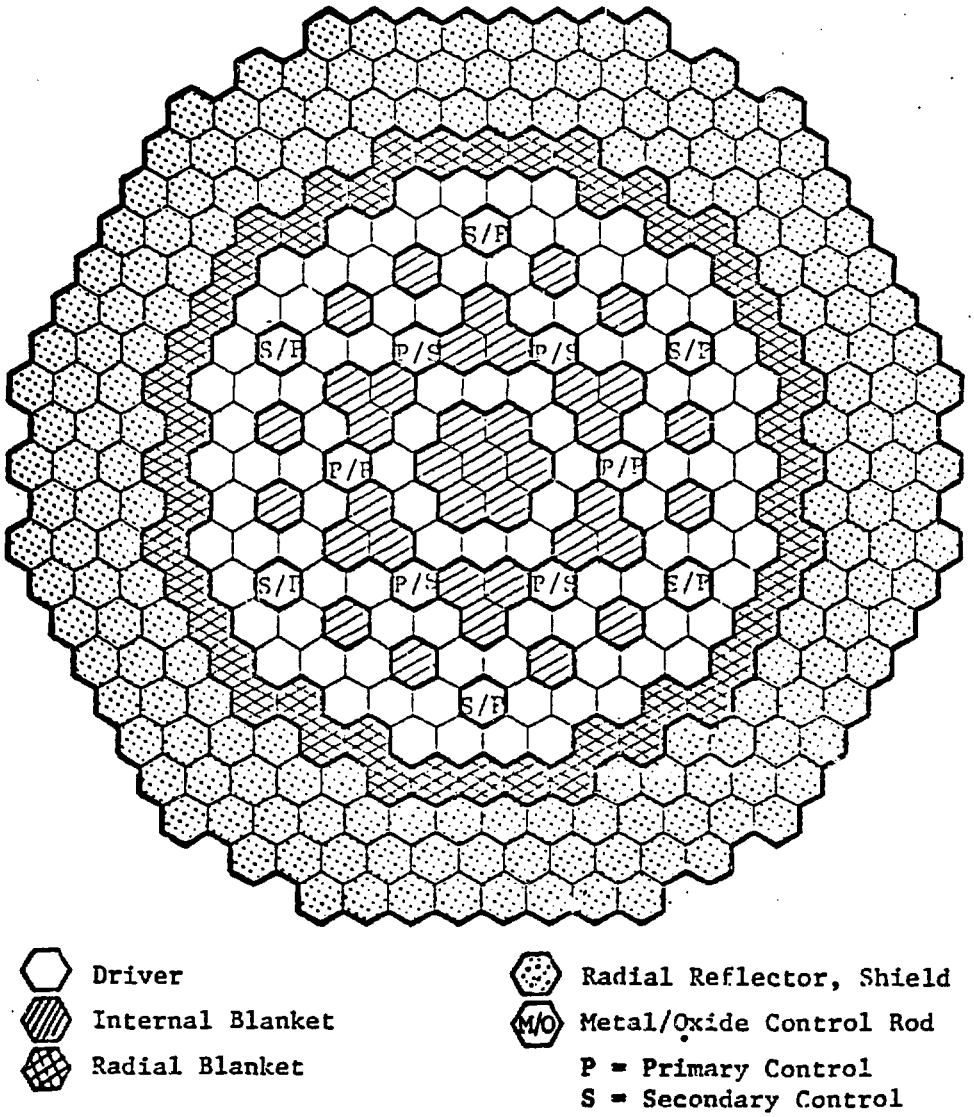

Fig. 1. Core Layout for Metal Fuel

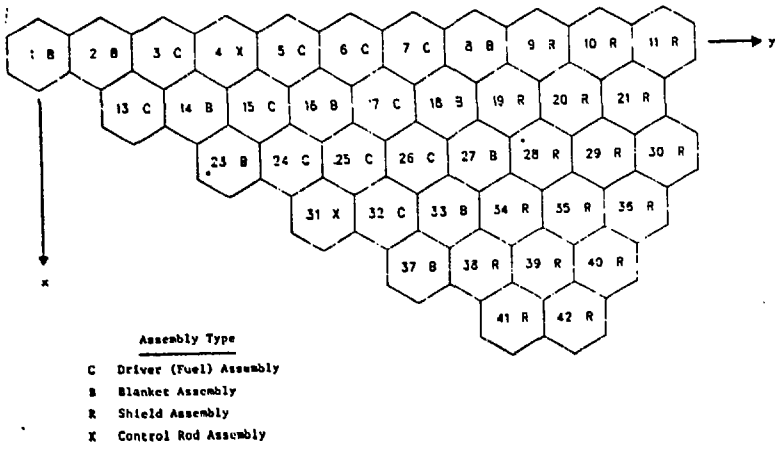

Fig. 2. 30-Degree Sector of Reactor Core

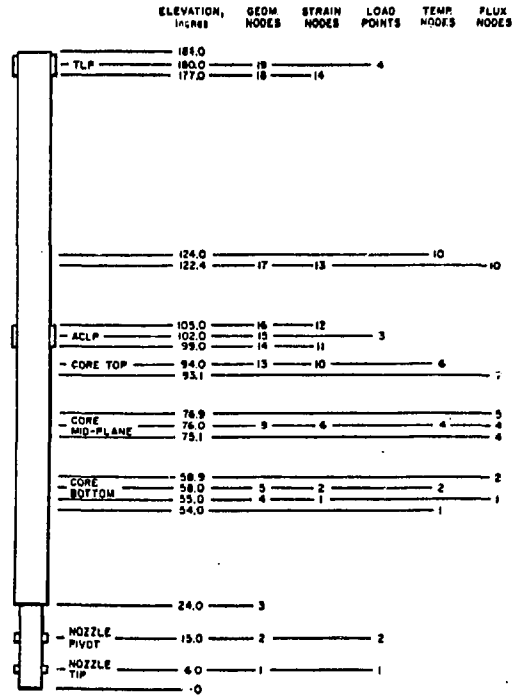

Fig. 3. Assembly Model Description in Vertical Direction

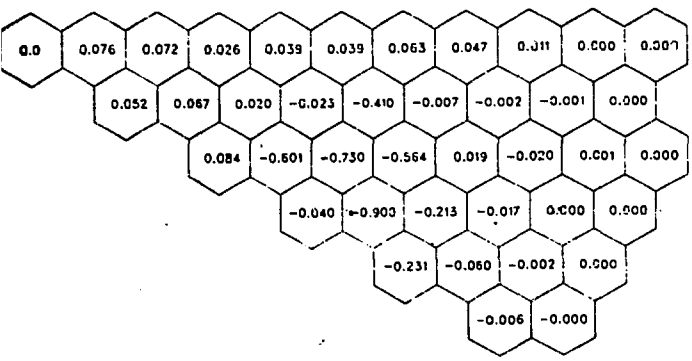

Fig. 4a. Assembly Displacement-Reactivity-Worths in x-Direction at Core Mid-Plane. (cents/in/in)

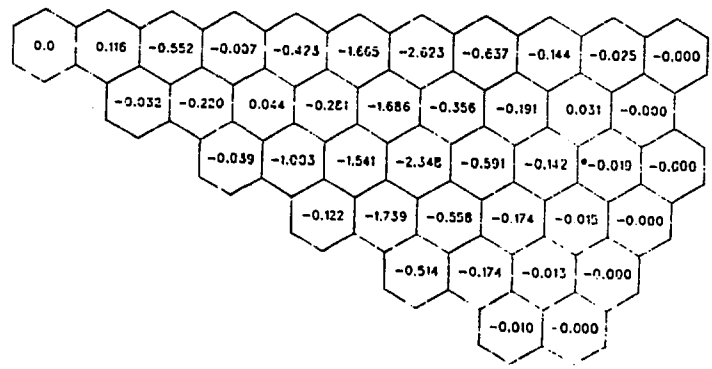

Fig. 4b. Assembly Displacement-Reactivity-Worths in y-Direction at Core Mid-Plane. (cents/in/in)

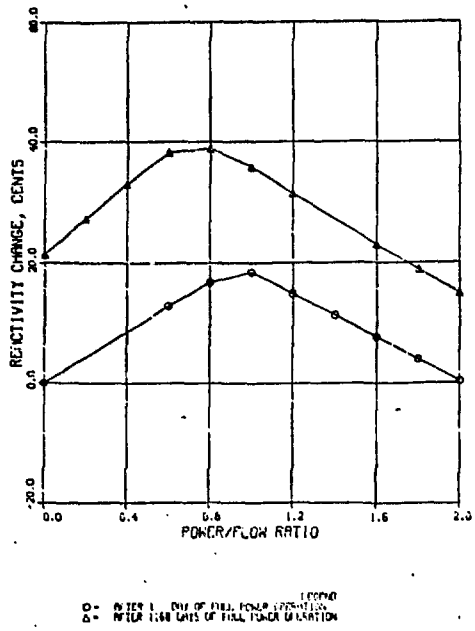

Fig. 5a. Bowing Reactivity Change Versus Power-to-Flow Ratio with Limited-Free-Bowing Restraint System

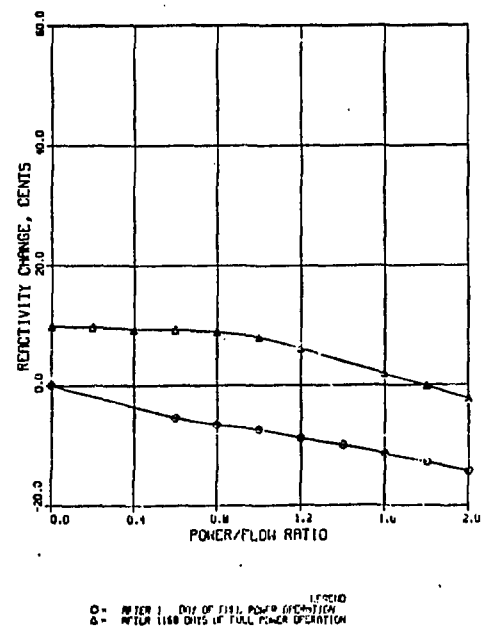

Fig. 5b. Bowing Reactivity Change Versus Power-to-Flow Ratio with Free-Flowering Restraint System

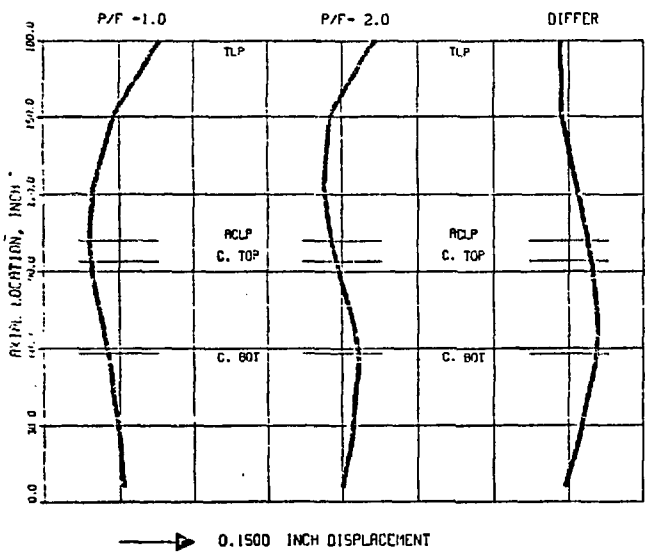

Fig. 6a. Radial Displacement of Assembly 7 at BOEC with Limited-Free-Bowing Restraint System

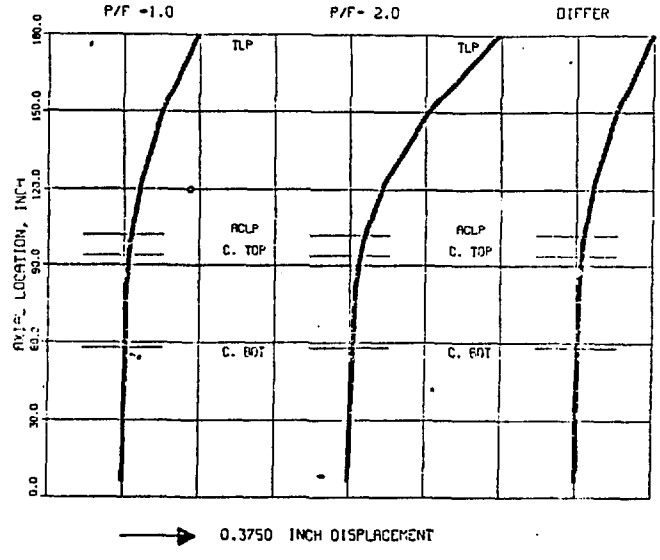

Fig. 6b. Radial Displacement of Assembly 7 at BOEC with Free-Flowering Restraint System

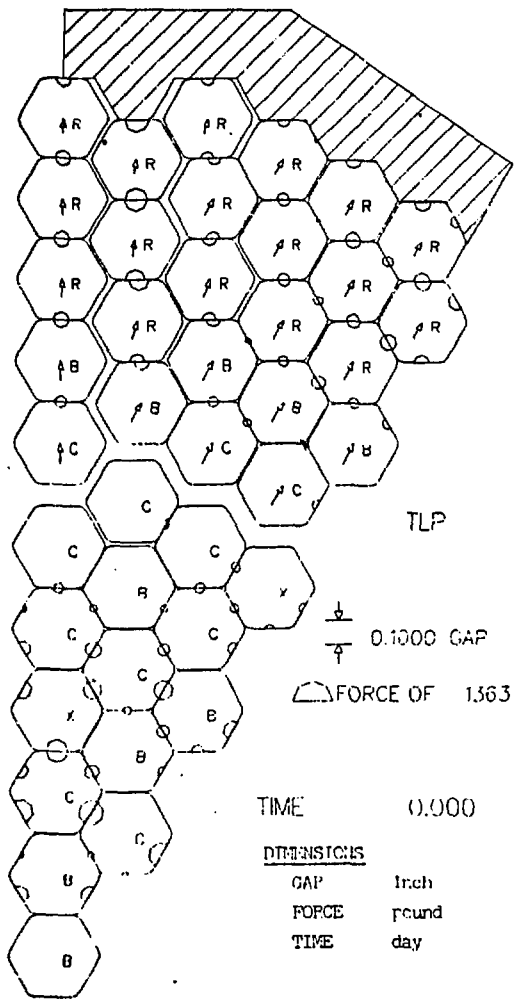

Fig. 7a. TLP Forces and Displacements at BOEC with Limited-Free Bowing Restraint System

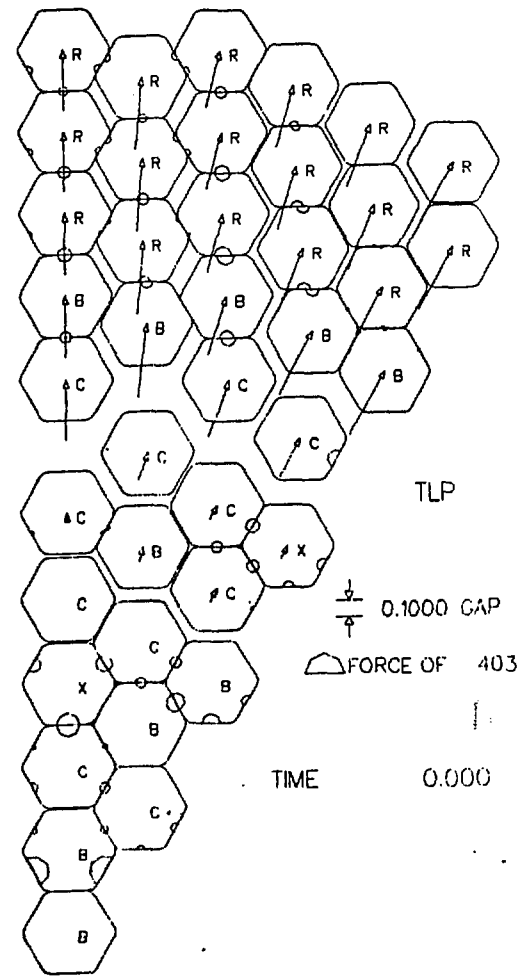

Fig. 7b. TLP Forces and Displacements at BQEC with Free-Flowering Restraint System

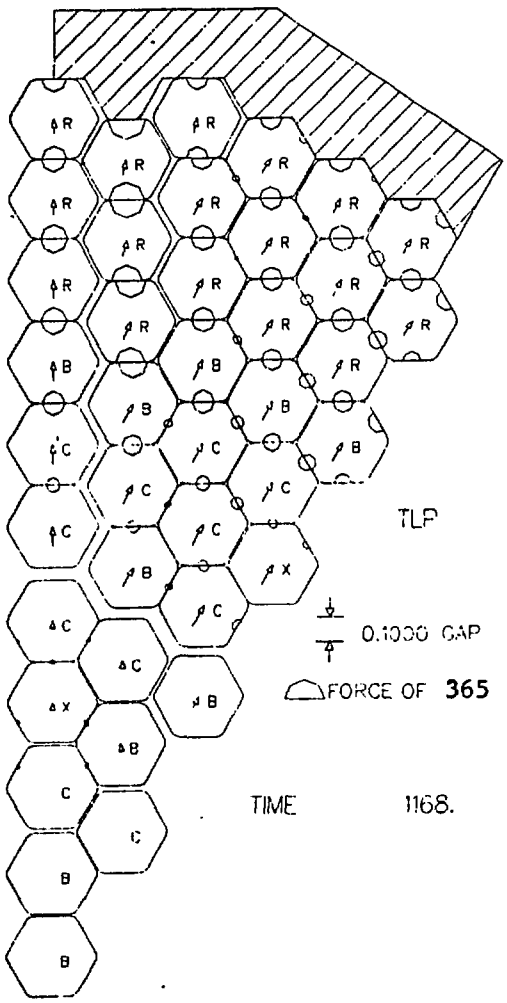

Fig. 8a. TLP Forces and Displacements at EOEC with Limited-Free-Bowing Restraint System

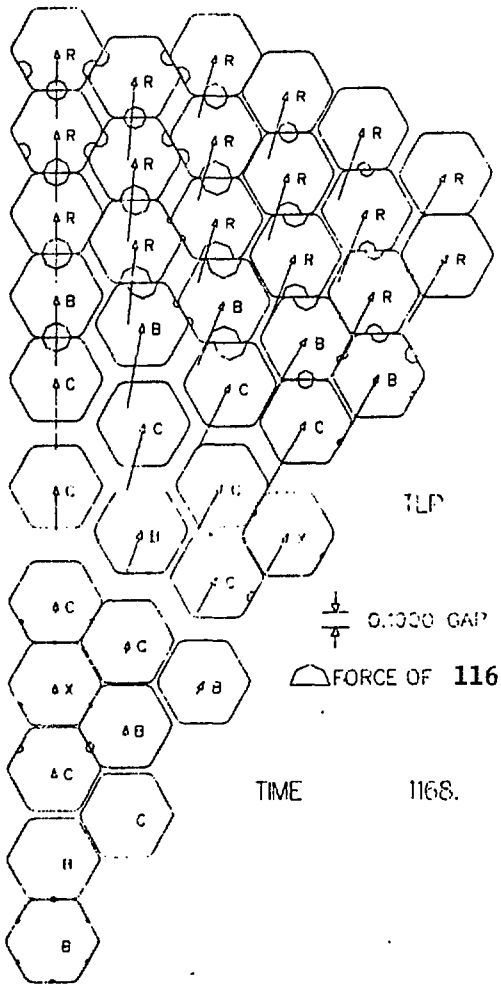

Fig. 8b. TLP Forces and Displacements at EOEC with Free-Flowering Restraint System